



Evaluation and optimization of textile synthetic effluent discoloration using anodic oxidation on BDD electrode: application of the experimental design methodology

Nour El Houda Abdessamad*, Hanène Akrou, Latifa Bousselmi

Waste Water Treatment Laboratory, Water Research and Technologies Center (CERTÉ), Echopark Borjcedria

Touristic Road of Soliman, BP 273, 8020 Soliman, Tunisia

Tel. +216 79 325 044; Fax: +216 79 325 802; email: nour_houda1@certe.rnrt.tn

Received 22 February 2012; Accepted 28 October 2012

ABSTRACT

In the present study, the anodic oxidation of an azoic dye Acid Orange 8 (AO8) was performed on boron-doped diamond electrode. Cyclic voltammetry of AO8 dye solution at pH 0 and 10 proved the existence of direct and indirect electrochemical reactions in the potential region between 1.0 and 2.3 V/saturated calomel electrode. A factorial design methodology was implemented to evaluate statistically the effects of operating parameters, including current intensity (0.1–0.6 A), initial pH (0–10), initial dye concentration (0.01–0.1 mmol L⁻¹), and electrolysis time (10–90 min), on discoloration efficiency. The equation describing the behavior of the response function of the selected factors was developed and verified by different tests such as ANOVA. The optimized parameters determined in this study were set as follows: current intensity of 0.35 A, initial pH=0, initial dye concentration of 0.055 mmol L⁻¹, and electrolysis time of 45 min. Under these conditions, 98% of discoloration efficiency was obtained. The anodic oxidation of AO8 was found to follow pseudo-first-order reaction kinetics, and also an apparent rate constant (k_{app}) of 0.082 min⁻¹ was found. The chemical oxygen demand was reduced by 70%.

Keywords: Anodic oxidation; BDD electrode; COD; Discoloration; Experimental design methodology; Optimization

1. Introduction

In textile industry, the release of wastewater containing dyes constitutes one of the most critical environmental problems [1]. Conventional methods such as biological, physical, and chemical processes commonly used on textile wastewater treatment are not able to mineralize completely pollutant with recalcitrant compounds groups [2–4]. Recently, the use of advanced oxidation processes (AOPs) such as photo-

catalytic degradation [5], catalytic ozonation [6], anodic oxidation [2,7], and electro-Fenton [8,9] has showed a promoting solution to treat this contaminated wastewater. All these treatments are attractive thanks to their efficiency in detoxifying and mineralizing hazardous bio-refractory organic compounds including dyes [10–12]. Anodic oxidation can be used as a pretreatment before the biological process to increase biodegradability of wastewater or it can be as a posttreatment that allowed the total mineralization of pollutants. This process is based on highly signifi-

*Corresponding author.

cant in situ electrogeneration of a powerful oxidant which is a radical hydroxyl OH^\bullet ($E^0 = 2.8 \text{ V/ENH}$ in aqueous solution at 25°C) [13]. These radicals are produced at the surface of a high O_2 -overvoltage anode from the oxidation of water, and react unselectively at a very high rate (k in the range of 10^7 – $10^{10} \text{ M}^{-1} \text{ s}^{-1}$) with a wide range of organic compounds leading to their mineralization [14].

Several anodes Pt, PbO_2 , doped PbO_2 , doped SnO_2 , and IrO_2 are employed in anodic oxidation [9]. Most of these electrodes have a short service life and release toxic ions [15]. Many studies have shown that the electrochemical oxidation of organic contaminants on boron-doped diamond (BDD) anodes can achieve a great efficiency compared to other anodes used [11,16]. This has been related to these desirable properties such as a great chemical and electrochemical stability which enhance the average lifetime, high resistance to corrosion, good electrical conductivity, and higher efficiency to electrogenerate radical hydroxyl OH^\bullet [8,17,18].

The electrochemical oxidation of dye solutions on BDD electrodes depends on several variables: initial dye concentration, initial pH solution, current density, temperature, flow rate as well as electrolysis time. The effect of these parameters on pollutants degradation is widely varying from one publication to another [2,9,19]. Two ways can be used to evaluate the effect of variables studied [19,20]. The most commonly used method involves the variation of one variable while keeping the other constant, until all variables are studied [21]. However, this may require a large number of experiments and cannot identify the possible interactions between them. Experimental statistical design method can overcome this shortcoming. By using this methodology, it was possible to investigate the influence of each parameter, to estimate the possible interaction effects of the factors, to design and construct a prediction model for the response, and to optimize the result desired with relatively small number of experiments [22–24]. It has been successfully applied to different AOPs including TiO_2 -coated [25] UV/ TiO_2 photo-catalytic process [26,27], electro-Fenton [28–30], and electrocoagulation [31], although, few papers have been focused on the application of the design methodology in anodic oxidation of dye solution on BDD electrodes.

In this paper, we have studied the anodic oxidation of Acid orange 8 (AO8) solutions on BDD electrode by cyclic voltammetry. The effect of different parameters on color removal of dye solution under galvanostatic mode was also investigated by using an efficient statistical approach based on a factorial experimental design. The first part of this study deals with (i) evaluating the effect of various operating

conditions including current intensity (I), initial pH, initial dye concentration (C_{AO8}^0), and electrolysis time (t_{elec}) and the effect of the interaction between them on color removal of dye solution, (ii) determining the statistical significance of each parameter, and (iii) constructing and verifying a model which can describe the functional relationship between a response and variables. The second part deals with finding optimal treatment conditions to completely achieve discoloration.

2. Experimental

2.1. Pollutant dye

The oxidation process was investigated using (AO8, $\text{C}_{17}\text{H}_{13}\text{N}_2\text{NaO}_4\text{S}$; MW $364.35 \text{ g mol}^{-1}$) as a model of a mono azoic dye. It was obtained from Aldrich in 65% purity and used without further purification. Azo dyes which contain a hydroxyl group conjugated with the azo linkage exist as an equilibrium mixture of two tautomeric forms, azo or hydrazone [32].

Many studies have proved that when the hydroxyl group is positioned in a naphthol ortho to the azo group, the equilibrium favored the hydrazone form, particularly in aqueous medium [33,34]. They have also demonstrated that the hydrazone form is bathochromic compared with the azo form and usually have usually a higher tinctorial strength.

Moreover, we have to take into consideration another equilibrium since the hydroxyl groups in azo dyes have pK_a values of 1 (of the $-\text{SO}_3\text{H}$ group) and 11.4 (of naphthalene oxygen group) [9,35]. Accordingly, depending on the pH media, different species might be appearing.

In this study, experiments were conducted in aqueous medium at pH strongly acid ($\text{pH}=0$) and $\text{pH}=10$. The UV–visible spectra of AO8 solution from 200 to 600 nm at different pHs is shown in Fig. 1.

On basic medium, the spectrum of AO8 in the visible region exhibited a main band with a maximum of 480 nm and a shoulder of 410 nm. The absorption band at 480 nm revealed the presence of the hydrazone form, whereas the shoulder at 410 nm indicated the presence of the azo form. The other peaks, located at 230, 260, and 310 nm were due to the π – π^* transition of the aromatics compounds bonded to the azo group in the dye molecule [34]. In strongly acidic medium, a hypsochromic shift ($\lambda = 395 \text{ nm}$) could be noticed. The absorption band in the visible region is restricted. Nevertheless, in both cases, the coloration of the initial dye solution is orange. The difference of the absorption spectra of AO8 confirmed that the behavior of AO8 depended on pH medium which defined the predominated species in solution.

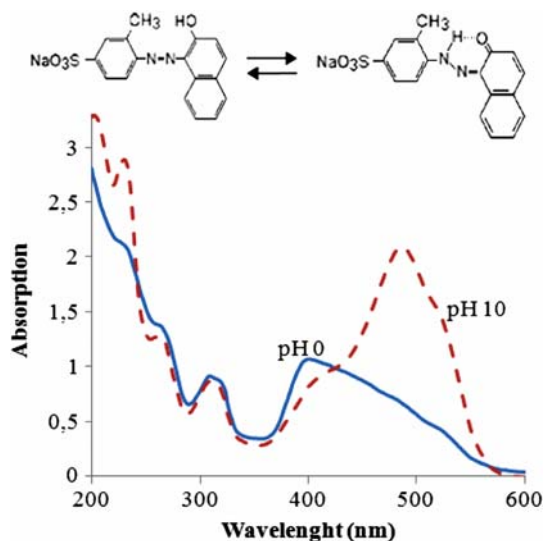


Fig. 1. Absorption spectra of AO8 (0.1 mmol L^{-1}) and Na_2SO_4 (0.1 mol L^{-1}) at pH 0 and pH 10. Inset: chemical structure of AO8 in the tautomeric equilibrium.

2.2. Electrochemical experiments

Electrolyses were conducted in a mini DiaCell (type PS 500) single compartment electrolytic cell with parallel plate electrodes manufactured by Adamant Technologies. The anode is a monopolar Si/BDD and the cathode is a stainless steel. The active surface is 12.5 cm^2 and the electrode gap is 3 mm.

Before each experiment was carried out, the BDD electrode was subjected to auto cleaning procedure in H_2SO_4 (1 M) for 30 min. This cleaning is essential for the regeneration of anode because it can remove any possible organic polymer formed at the electrode surface causing reactivity failing [36]. A washing with distilled water is recommended to neutralize the medium. All experiments were performed under galvanostatic mode. The dye solution was stored in a glass tank (1 L) and circulated through the electrolytic cell by means of a peristaltic pump working in recycling mode. The flow rate is fixed at 3.38 L min^{-1} and the temperature at 25°C .

Sulfuric acid (96%) and sodium hydroxide (100%) were provided by Merck. Distilled water was used throughout for the preparation of aqueous solutions. From an economical and environmental point of view, the Na_2SO_4 (99.5%) is one of the commonly supporting electrolytes used in the anodic oxidation process. Therefore, Na_2SO_4 at 0.1 mol L^{-1} was selected as the support electrolyte in this work. The electrolytic medium was made basic or acidic as required by the addition of aqueous NaOH (0.1 mol L^{-1}) or H_2SO_4 (0.1 mol L^{-1}), respectively.

2.3. Analytic procedure

Samples were withdrawn from the reactor at a desired time, and the discoloration efficiency was evaluated by following the drop of the absorbance of the AO8 solution at the maximum visible wavelength λ_{max} (485 nm at pH 10 and 395 nm at pH 0) measured on a UV/visible spectrophotometer (Thermospectronic UV1).

To assess the progress of AO8 mineralization, the chemical oxygen demand (COD) removal was determined by an open reflux, dichromate titrimetric method as described in Standard Methods [37].

2.4. Voltammetry experiments

All electrochemical measurements were performed in a single-compartment three-electrode glass cell, by using a Radiometer PGZ 301 potentiostat, which was interfaced to a computer running VoltaMaster4 software.

A saturated calomel electrode (SCE) was used as the reference and platinum served as the auxiliary electrode. The BDD was used as the working electrode (0.237 cm^2). The BDD electrode was anodically polarized for 2 min at 2.5 V in $1 \text{ mol L}^{-1} \text{ H}_2\text{SO}_4$ prior to each experiment [18,38].

2.5. Experimental design methodology

The chemometric approach was performed using a central composite design (CCD). The analysis of the experimental data was supported by the STATISTICA Software system.

Four main independent variables that would affect treatment efficiency were taken into account: current intensity (U_1), initial dye solution pH (U_2), initial dye concentration (U_3), and electrolysis time (U_4). Each one of the four independent variables received two values: a high value (indicated by the +1) and a low value (indicated by the -1). Four repeat runs were also performed at the center of the design (mean value indicated by zero) in order to estimate the standard error. The experimental design is presented in Table 1.

The appropriate selection of experimental domain for each factor was made from prior knowledge of our electrochemical system, results of other research, and the performances of electrochemical reactor used.

The central composite design consisted of 28 experiments divided into three blocks: (a) a full factorial design 2^4 (all possible combinations of codified values +1 and -1); (b) 8 (2×4) axial points located at the center and both extreme levels; and (c)

Table 1
Experimental region investigated for the AO8 discoloration

Coded Variables	Independent variable (U_i)	Unit	Experimental field		
			Low levels (–1)	Center level (0)	High levels (+1)
X_1	U_1 : current intensity	A	0.1	0.35	0.6
X_2	U_2 : initial pH		0	5	10
X_3	U_3 : initial dye concentration	mmol L ⁻¹	0.01	0.055	0.1
X_4	U_4 : electrolysis time	min	10	50	90

four central replicates of the central points, as shown in Table 2. It also showed actual experimental responses (Y_{exp}) corresponding to discoloration efficiency and determined by the following expression:

$$\text{Discoloration efficiency (\%)} = \frac{A_0 - A_t}{A_0} \times 100 \quad (1)$$

where A_0 and A_t are the absorbance before electrolysis and after an electrolysis time t , respectively, at maximum band intensity.

The response variable was fitted by a second-order model. The general form of the second-degree polynomial equation is:

$$Y = b_0 + \sum_{i=1}^{i=4} b_i X_i + \sum_{j=1}^4 b_{jj} X_j^2 + \sum_i \sum_{j=2}^{i=4} b_{ij} X_i X_j \quad (2)$$

where Y represents the experimental response (discoloration efficiency); b_0 is an independent term; b_i represents the coefficients of the linear terms; b_{jj} and b_{ij} are the coefficients corresponding to the interaction term between the factor i and the factor j of quadratic and the second-order terms, respectively, and X_i is the coded variables (–1 or +1). This expression is preferred because a relatively few experimental combinations of the variables are adequate to estimate potentially complex response function [39].

The validation of the model was studied by the determination of the coefficient R^2 , the calculation of the residuals, and the estimation of the standard error and the ANOVA tests.

3. Results and discussion

3.1. Cyclic voltammetry

In order to obtain more information concerning the oxidative mechanisms of the AO8 molecule on BDD electrode, voltammetric measurements were carried out.

Fig. 2 shows the cyclic voltammograms obtained with a scan rate of 0.1 V s⁻¹ in the potential region between 0.5 and 2.3 V/SCE of aqueous solutions of AO8 (0.01 mmol L⁻¹) in the presence of Na₂SO₄ as supporting electrolyte (0.1 mol L⁻¹) at pH 0 and 10.

The inset in Fig. 2 shows the cyclic voltammogram of the support electrolyte without AO8 dye at the same conditions at pH 0 and 10. We can see that the two cyclic voltammograms are superimposed, reflecting the negligible effect of pH on anodic oxidation of sulfate. A same anodic peak at 2.3 V/SCE was observed. This peak was attributed to the generation

of radical hydroxyl by oxidation of water as the following equation (Eq. (3)).



Compared to the voltammograms of support electrolyte, the electrochemical ability of AO8 on BDD electrode was evidenced from the appearance of anodic peaks attributed to its oxidation in two media. As can be observed, the voltammograms of AO8 dye solution in strongly acidic media lead to the appearance of two anodic oxidation peaks at approximately 1.01 V/SCE (P_1) and 1.82 (P_2) V/SCE. At pH 10, more oxidative peaks are obtained. It can be seen that the presence of three oxidative peaks is at about 1.04 V/SCE (P_3), 1.35 V/SCE (P_4), and 1.89 (P_5) V/SCE. This result suggested that more by-products are formed during the oxidation of AO8 dye in basic medium. Also, the difference in the shape of cyclic voltammograms confirmed the presence of different species at each solution pH.

The peaks noted P_1 and P_3 observed in the zone of the stability of electrolyte indicated the existence of direct electrochemical reactions in this potential region. The shoulder peaks observed at values of potential close to that of water decomposition (P_2 , P_4 , and P_5) can be explained by an indirect oxidation process mediated by the oxidants electrogenerated by the surface of BDD electrode [11]. In fact, in the literature, it is well known that the high oxidation power of BDD favors the generation of hydroxyl radical as well as other weaker species, such as the peroxy derivatives coming from the oxidation of the anion of the supporting electrolyte. For instance, the peroxydisulfate ($\text{S}_2\text{O}_8^{2-}$) results from the sulfate oxidation can participate in the degradation of organic compounds [18].

As the number of cycle increases, the anodic current peaks decrease (not shown). The values of anodic peaks (P_1 and P_2) for the fourth cycle are reduced, respectively, at about 20 and 50%. This decrease is explained by many authors by the formation of organics passivating the films at the surface of BDD electrode [2,15,18]. In order to regenerate BDD, an anodic polarization at 2.5 V/ESC was imposed for 2 min in H_2SO_4 (1 mol L⁻¹). At this potential, the oxidation of water leads to the formation of significant amounts of hydroxyl radicals that react rapidly with the organics at the surface of the anode leading to their total mineralization and activating the surface once again. This fact was verified as cycle 5 after reactivity and, the first scan are nearly superimposed; this indicates the complete reactivation of the BDD electrode surface in these conditions.

The cyclic voltammograms were recorded on BDD electrodes in the presence of AO8 at different concentrations (0.1–0.8 mmol L⁻¹) at pH 0 and are shown in Fig. 2.

It is clearly seemed in Fig. 2 the dependence of the current density to the amount of dye in solution. Linear regressions of 0.99 are obtained. This result suggested that the oxidation of AO8 dye solution behaved as a mass-transfer-controlled process. The electrochemical oxidation of AO8 dye at BDD electrode was proved by the voltammetric study, in the next part, the influence of process factors on the

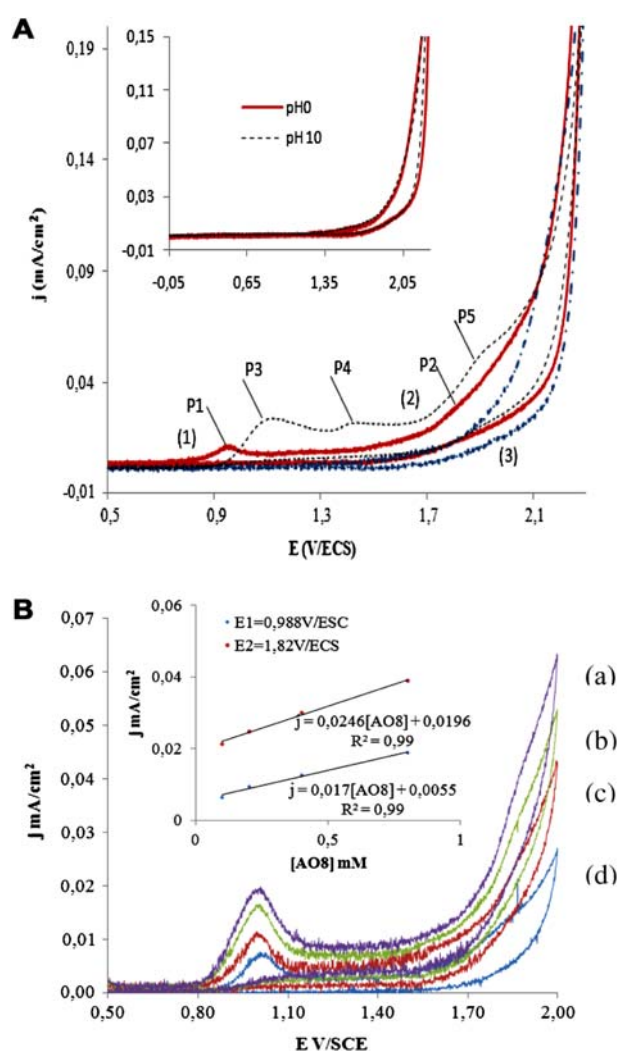


Fig. 2. Cyclic voltammograms of AO8 (A) (0.1 mmol L⁻¹) solutions on BDD electrode at (1) pH 0, (2) pH 10, (3) without AO8. Inset: Cyclic voltammograms of 0.1 mol L⁻¹ Na₂SO₄ without AO8 dye; (B) (a) 0.1, (b) 0.2, (c) 0.4 and (d) 0.8 mmol L⁻¹ AO8 at pH = 0. Inset: Evolution of current density versus dye concentration.

discoloration dye solution was carried out under galvanostatic mode using the experimental design approach to determine the optimum conditions.

3.2. Bulk electrolysis

3.2.1. Effect of the operating parameters on the discoloration efficiency using the experimental design methodology

Statistical analysis of the response factors involved the estimation of the average effect, the main effects of each individual variable, as well as their two and higher order interaction effects. A mathematical equation (Eq. (4)) that described the functional relationship between a response *Y* (discoloration efficiency) and a set of independent variables (i.e. current intensity (*U*₁), initial dye solution pH (*U*₂), initial dye concentration (*U*₃), and electrolysis time (*U*₄)) was determined.

$$\begin{aligned}
 Y_1 = & 53.70 + 9.94X_1 - 6.25X_1^2 - 15.2X_2 + 19.93X_2^2 \\
 & - 13.44X_3 + 16.99X_3^2 + 26.53X_4 - 24.23X_4^2 \\
 & + 2.64X_1X_2 - 1.37X_1X_3 - 3.25X_1X_4 \\
 & + 2.78X_2X_3 + 0.85X_2X_4 + 4.56X_3X_4 \quad (4)
 \end{aligned}$$

The Pareto analysis (Fig. 3) gives more significant information to interpret the results. It allowed to visualize the importance of the calculated factors in (Eq. (4)) and to check the weight of the different coefficients.

All estimated effects greater than *P*-value=0.05 (95% confidence intervals) are considered significant. Hence, Pareto graphic analysis showed that the most important parameters influenced discoloration efficiency were the electrolysis time and the initial pH

followed by initial dye concentration and current intensity.

Positive and negative effects indicated, respectively, synergistic effect and antagonistic effect.

Then, the discoloration efficiency increased with the increase of current intensity and electrolysis time revealing positive effect while decreasing at basic pH and high dye concentrations. Furthermore, it was noted the important positive interaction between initial dye concentration and electrolysis time with a contribution of 17.2% indicated a synergetic effect between them.

The effect of initial pH can be explained by the differences observed in UV–visible analyses and cyclic voltammograms of the AO8 solution at two pHs investigated (Sections 2.1 and 3.1). Thus, it can be said that the form predominated in strongly acidic medium is more easily oxidized than the form present in basic media. On the other hand, the pH value may influence the amount of hydroxyl radicals produced. This strong oxidant, more generated in acidic medium, can destroy quickly and nonselectively most of the organic matter present in water sample.

The negative effect of the initial dye concentration can be assigned as follows. The discoloration efficiency was related to the probability of OH· radicals formation and to their probability to react with dye molecules. Then, at the high dye concentration, amount of hydroxyl radical will not be enough to discoloration of high concentration pollutant and removal efficiency decreases. This result agrees with many research works [40].

3.2.2. Validation of model

The quality of the fit of the quadratic model was checked by the determination of the coefficient regression *R*², calculation of the residuals, estimation of the standard error and by the ANOVA tests. In this study, the experimental design was modeled by Eq. (4) with *R*²=0.899. This implied that 89.90% of the variations for dye discoloration efficiency were explained by the independent variables and this also means that the model does not explain only 10.1% of variation. This result indicates that the second-order polynomial model (Eq. (4)) was significant. This good fitness can be improved also by calculated residuals (difference between the observed and the predicted response values) as shown in Table 2.

To assess the significance of the effects, an estimate of the standard error is required. Standard error for this model was calculated at a value of 1.13. If an

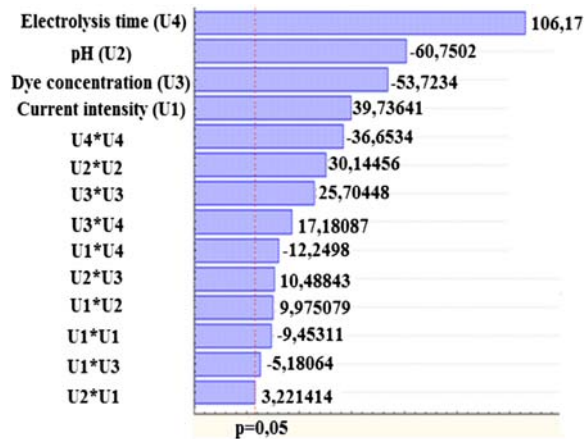


Fig. 3. Graphical Pareto analysis.

Table 2
Factorial experimental design, experimental plan, and results

Experiment number	Experimental design			Experimental plan			Results		
	X_1	X_2	X_3	U_1	U_2	U_3	U_4	Y_1 exp(%)	Residuals
1	-1	-1	-1	-1	0	0.01	10	56.11	-2.43
2	+1	-1	-1	-1	0	0.01	10	97.25	14.87
3	-1	+1	-1	-1	10	0.01	10	7.17	-8.39
4	+1	+1	-1	-1	10	0.01	10	38.13	-11.86
5	-1	-1	+1	-1	0	0.1	10	8.44	-11.27
6	+1	-1	+1	-1	0	0.1	10	30.52	-7.54
7	-1	+1	+1	-1	10	0.1	10	6.71	18.84
8	+1	+1	+1	-1	10	0.1	10	23.66	6.85
9	-1	-1	-1	+1	0	0.01	90	100	-7.27
10	+1	-1	-1	+1	0	0.01	90	100	-18.11
11	-1	+1	-1	+1	10	0.01	90	75.98	8.27
12	+1	+1	-1	+1	10	0.01	90	100	10.86
13	-1	-1	+1	+1	0	0.1	90	99.28	12.59
14	+1	-1	+1	+1	0	0.1	90	100	7.98
15	-1	+1	+1	+1	10	0.1	90	42.98	-15.28
16	+1	+1	+1	+1	10	0.1	90	77.35	3.16
17	0	0	0	0	5	0.055	50	55.07	4.94
18	0	0	0	0	5	0.055	50	55.84	-6.21
19	0	0	0	0	5	0.055	50	54.38	11.17
20	0	0	0	0	5	0.055	50	53.34	-12.44
21	-1	0	0	0	5	0.055	50	42.45	14.06
22	+1	0	0	0	5	0.055	50	51.19	-15.33
23	0	-1	0	0	0	0.055	50	100	0.93
24	0	+1	0	0	10	0.055	50	45.99	-2.204
25	0	0	-1	0	5	0.01	50	98.20	1.366
26	0	0	+1	0	5	0.1	50	41.92	2.14
27	0	0	0	-1	5	0.055	10	3.88	0.68
28	0	0	0	+1	5	0.055	90	53.80	-0.36

Table 3
ANOVA test for response function Y

	Error type	Sum of square	Mean square	F-value	p-value (Prob > F)
Current intensity (U_1)	0.250232	1779.66	1779.66	1578.98	0.000035
$U_1 \times U_1$	0.661024	100.72	100.72	89.36	0.002509
pH (U_2)	0.250232	4159.63	4159.63	3690.59	0.000010
$U_2 \times U_2$	0.661024	1024.18	1024.18	908.69	0.000080
Dye concentration (U_3)	0.250232	3253.02	3253.02	2886.21	0.000014
$U_3 \times U_3$	0.661024	744.69	744.69	660.72	0.000129
Electrolyse time U_4	0.250232	12668.08	12668.08	11239.61	0.000002
$U_4 \times U_4$	0.661024	1514.21	1514.21	1343.47	0.000045
$U_4 \times U_2$	0.265411	112.15	112.15	99.50	0.002144
$U_4 \times U_3$	0.265411	30.25	30.25	26.84	0.013962
$U_4 \times U_1$	0.265411	169.13	169.13	150.06	0.001172
$U_2 \times U_3$	0.265411	123.99	123.99	110.01	0.001851
$U_2 \times U_1$	0.265411	11.70	11.70	10.38	0.048532
$U_3 \times U_1$	0.265411	332.70	332.70	295.18	0.000430
Manque adjust	0.367098	2841.23	284.12	252.09	0.000369

effect is about or below the SE, as this case, it may be considered insignificant [30,41].

The ANOVA test is used also to check the significance of the equation with the experimental data. This analysis included the Fisher's *F*-test. This test verified that the model is highly significant ($F_{\text{model}} = 252.09$). The probability *P*-value (Prob > *F*) is lesser than 0.0500 indicated that model terms are significant, whereas values greater than 0.1000 are not significant (Table 3).

According to the above observations, it can be concluded that the model is highly significant and experiments are highly accurate and reliable. This result confirmed that the predicted model can be applied to the CCD.

3.3. Determination of optimal conditions for the discoloration efficiency of AO8

The main objective of statistical software based on CCD [41,42] is to optimize the response surface that is influenced by process parameters. Each contour diagram plot has an infinite number of combinations based on two selected parameters while maintaining the two other factors constant at their middle values. Fig. 4(a–d) showed the response surface plot and the contour plots drawn vs. the main factors electrolysis time, pH, initial dye concentration, and current intensity.

The analyses of these graphics confirm preceding results. The increase of the current intensity results in a significant increase of color removal. It increases in the region from 0.3 to 0.65 A, but it decreases beyond 0.65 A. The maximum of discoloration efficiency was obtained where the treatment time increased and the initial pH and initial dye concentration decreased.

Accordingly, the optimal working conditions were obtained at 45 min of treatment of a 0.055 mmol L⁻¹ AO8 solution at a current intensity maintained at 0.35 A in strongly acidic media. These conditions led to maximum discoloration efficiency at 98%. The kinetic analysis of the reaction between AO8 and hydroxyl radicals showed that the anodic oxidation of AO8 on BDD electrode fitted with a pseudo-first-order model. This finding suggested that during electrolysis time, radical hydroxyl produced by anodic oxidation reached a steady state. The pseudo-first-order rate constant ($k_{\text{app}} = 0.082 \text{ min}^{-1}$) was determined from the slope of the plot $\ln [\text{AO8}]_t / [\text{AO8}]_0$. Moreover, under the optimum conditions, 70% of AO8 mineralization, evaluated through COD measurement, was achieved (not shown). These results confirmed that the anodic oxidation of AO8 in strongly acidic media favored a rapid degradation of azo group as the most active site for oxidative attack of AO8 molecule by hydroxyl radicals electrogenerated. The intermediates generated during AO process were oxidized more slowly. The contribution of hydroxyl radicals in AO confirms the results obtained from cyclic voltammetry which prove that the oxidation process of AO8 on BDD electrode was mediated by OH[•].

4. Conclusions

In this study, the electrochemical oxidation of AO8 dye at BDD electrode was proved by the cyclic voltammetry study. A factorial experimental design was adopted to investigate the effects of four main factors, which were current intensity, initial pH, initial dye concentration, and electrolysis time on the discolor-

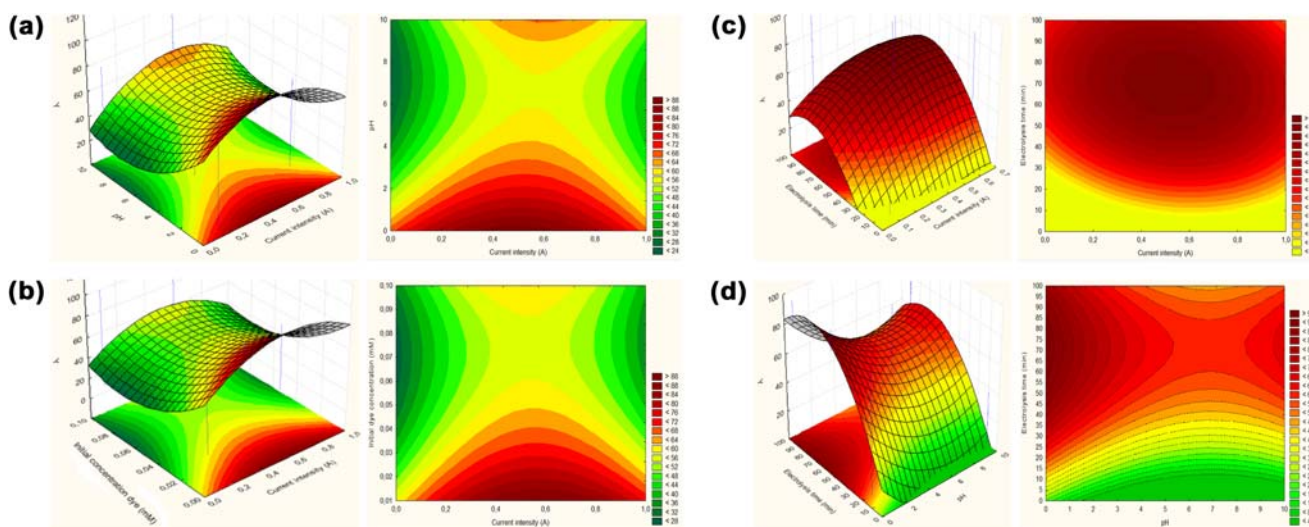


Fig. 4. Response surface plot and contour plots of color removal vs. the main factors: (a) pH and current intensity: $[AO8] = 0.055 \text{ mmol L}^{-1}$ and electrolysis time = 50 min. (b) Initial dye concentration and current intensity: electrolysis time = 50 min, pH 5. (c) Electrolysis time and current intensity: $[AO8] = 0.055 \text{ mmol L}^{-1}$, pH 5. (d) Electrolysis time (min) and pH: $[AO8] = 0.055 \text{ mmol L}^{-1}$, current intensity = 0.35 A.

ation of AO8 solution by anodic oxidation on BDD electrode. Electrolysis time and initial pH were found to have the most significant effects followed by initial dye concentration and current intensity. Agreement of the quadratic models with the experimental data was satisfactory. Thus, central composite design was adopted to determine the optimum experimental conditions, which were found $I = 0.35 \text{ A}$, $\text{pH}^0 = 0$, $C_{AO8}^0 = 0.055 \text{ mmol L}^{-1}$, and $t_{\text{elec}} = 45 \text{ min}$. Under these conditions, 98% of discoloration efficiency and 70% of COD removal were achieved. The pseudo-first-order rate constant (k_{app}) of the reaction between AO8 and hydroxyl radicals during anodic oxidation processing was determined as 0.082 min^{-1} .

Acknowledgments

This research was done with the support of International Foundation for Science (IFS), Sweden, by a research fellowship to CP: HaneneAkrouit-Baccour.

Authors acknowledge also Capacity Building for Direct Water Reuse in the Mediterranean Area (CB-WR-MED) project financed by EU under Seventh Framework Programme (FP7) and contract objective project financed by Ministry of Higher Education and Scientific Research in Tunisia.

References

- [1] M.M. Fazli, A.R. Mesdaghinia, K. Naddafi, S. Nasser, M. Yunesian, M.M. Assadi, S. Rezaie, H. Hamzehei, Screening of factors affecting reactive blue 19 decolorization by *Ganoderma* sp. using fractional factorial experimental design, *Desalin. Water Treat.* 22 (2010) 22–29.
- [2] A.M. Faouzi, B. Nasr, G. Abdellatif, Electrochemical degradation of anthraquinone dye Alizarin Red S by anodic oxidation on boron-doped diamond, *Dyes Pigm.* 73 (2007) 86–89.
- [3] D. Rajkumar, B.J. Song, J.G. Kim, Electrochemical degradation of Reactive Blue 19 in chloride medium for the treatment of textile dyeing wastewater with identification of intermediate compounds, *Dyes Pigm.* 72 (2007) 1–7.
- [4] T.M. Elmorsi, Y.M. Riyad, Z.H. Mohamed, H.M.H. Abd El Bary, Decolorization of Mordant red 73 azo dye in water using $\text{H}_2\text{O}_2/\text{UV}$ and photo-Fenton treatment, *J. Hazard. Mater.* 174 (2010) 352–358.
- [5] R. Mu, Z. Xu, L. Li, Y. Shao, H. Wan, S. Zheng, On the photocatalytic properties of elongated TiO_2 nanoparticles for phenol degradation and Cr(VI) reduction, *J. Hazard. Mater.* 176 (2010) 495–502.
- [6] L.A. Bernal-Martinez, C. Barrera-Diaz, C. Solis-Morelos, R. Natividad, Synergy of electrochemical and ozonation processes in industrial wastewater treatment, *J. Chem. Eng.* 165 (2010) 71–77.
- [7] N. Abdessamad, N. Adhoum, Spontaneous adsorption and electrochemical behaviour of safranin O at electrochemically activated glassy carbon electrode, *Mater. Chem. Phys.* 116 (2009) 557–562.
- [8] C. Flox, S. Ammar, C. Arias, E. Brillas, A.V. Vargas-Zavala, R. Abdelhedi, Electro-Fenton and photoelectro-Fenton degradation of indigo carmine in acidic aqueous medium, *Appl. Catal. B: Environ.* 67 (2006) 93–104.
- [9] W.L. Chou, C.T. Wang, C.P. Chang, Comparison of removal of Acid Orange 7 by electrooxidation using various anode materials, *Desalination* 266 (2011) 201–207.
- [10] M.Y.A. Mollaha, P. Morkovsky, J.A.G. Gomes, M. Kesmez, J. Pargad, D.L. Cocke, Fundamentals, present and future perspectives of electrocoagulation, *J. Hazard. Mater. B.* 114 (2004) 199–210.
- [11] C. Saez, M. Panizza, M.A. Rodrigo, G. Cerisola, Electrochemical incineration of dyes using a boron-doped diamond anode, *J. Chem. Technol. Biotechnol.* 82 (2007) 575–581.
- [12] K. Cruz-Gonzalez, O. Torres-Lopez, A. Garcia-Leon, J.L. Guzman-Mar, L.H. Reyes, A. Hernandez-Ramirez, J.M. Peralta-Hernandez, Determination of optimum operating parameters for Acid Yellow 36 decolorization by electro-Fenton process using BDD cathode, *J. Chem. Eng.* 160 (2010) 199–206.

- [13] H. Akrouf, L. Bousselmi, Chlorides ions as agent promoting the oxidation of synthetic dyestuff on BDD electrode, *Desalin. Water Treat.* 46 (2012) 171–181.
- [14] A. Dhaouadi, N. Adhoum, Degradation of paraquat herbicide by electrochemical advanced oxidation methods, *J. Electroanal. Chem.* 637 (2009) 33–42.
- [15] H. Yining, Q. Jiuhui, Z. Xu, L. Huijuan, Electrochemical incineration of dimethyl phthalate by anodic oxidation with boron-doped diamond electrode, *J. Environ. Sci.* 21 (2009) 1321–1328.
- [16] R.E. Palma-Goyes, F.L. Guzman-Duque, G. Penuela, I. Gonzalez, J.L. Nava, R.A. Torres-Palma, Electrochemical degradation of crystal violet with BDD electrodes: Effect of electrochemical parameters and identification of organic by-products, *Chemosphere* 81 (2010) 26–32.
- [17] A. Kraft, M. Stadelmann, M. Blaschke, Anodic oxidation with doped diamond electrodes: A new advanced oxidation process, *J. Hazard. Mater.* B103 (2003) 247–261.
- [18] C.A. Martinez-Huitile, E. Brillas, Decontamination of wastewaters containing synthetic organic dyes by electrochemical methods: A general review, *Appl. Catal. B: Environ.* 87 (2009) 105–145.
- [19] B.K. Korbahti, Response surface optimization of electrochemical treatment of textile dye wastewater, *J. Hazard. Mater.* 145 (2007) 277–286.
- [20] Y. Lin, C. Ferronato, N. Deng, F. Wu, J.M. Chovelon, Photocatalytic degradation of methylparaben by TiO₂: Multivariable experimental design and mechanism, *Appl. Catal. B: Environ.* 88 (2009) 32–41.
- [21] A. Deligiorgis, N.P. Xekoukoulotakis, E. Diamadopoulou, D. Mantzavinos, Electrochemical oxidation of table olive processing wastewater over boron-doped diamond electrodes: Treatment optimization by factorial design, *Water Res.* 42 (2008) 1229–1237.
- [22] J. Goupy, L. Creighton, *Introduction Aux plans d'Expériences*, fourth ed., Dunod, Paris, 2001.
- [23] E. Chatzisyneon, N.P. Xekoukoulotakis, E. Diamadopoulou, A. Katsaounis, D. Mantzavino, S Boron-doped diamond anodic treatment of olive mill wastewaters: Statistical analysis, kinetic modeling and biodegradability, *Water Res.* 43 (2009) 3999–4009.
- [24] S. Kertész, J. Landaburu-Aguirre, V. García, E. Pongrácz, C. Hodúr, R. L. Keiski, A statistical experimental design for the separation of zinc from aqueous solutions containing sodium chloride and *n*-butanol by micellar enhanced ultrafiltration, *Desalin. Water Treat.* 9 (2009) 221–228.
- [25] P.J. Lu, C.W. Chien, T.S. Chen, J.M. Chern, Azo dye degradation kinetics in TiO₂ film-coated photoreactor, *J. Chem. Eng.* 163 (2010) 28–34.
- [26] H.L. Liu, Y.R. Chiou, Optimal decolorization efficiency of reactive red 239 by UV/TiO₂ photocatalytic process coupled with response surface methodology, *J. Chem. Eng.* 112 (2005) 173–179.
- [27] I.L. Cho, K.D. Zoh, Photocatalytic degradation of azo dye (Reactive Red 120) in TiO₂/UV system: Optimization and modeling using a response surface methodology (RSM) based on the central composite design, *Dyes Pigm.* 75 (2007) 533–543.
- [28] S. Hammami, N. Oturan, N. Bellakhal, M. Dachraoui, M.A. Oturan, Oxidative degradation of direct orange 61 by electro-Fenton process using a carbon felt electrode: Application of the experimental design methodology, *J. Electroanal. Chem.* 610 (2007) 75–84.
- [29] A.K. Abdessalem, N. Oturan, N. Bellakhal, M. Dachraoui, M. A. Oturan, Experimental design methodology applied to electro-Fenton treatment for degradation of herbicide chlortoluron, *Appl. Catal. B: Environ.* 78 (2008) 334–341.
- [30] K. Cruz-González, O. Torres-Lopez, A.M. García-León, E. Brillas, A. Hernández-Ramírez, J.M. Peralta-Hernández, Optimization of electro-Fenton/BDD process for decolorization of a model azo dye wastewater by means of response surface methodology, *Desalination* 286 (2012) 63–68.
- [31] N. Drouiche, S. Aoudj, H. Lounici, H. Mahmoudi, N. Ghafour, M.F.A. Goosen, Development of an empirical model for fluoride removal from photovoltaic wastewater by electrocoagulation process, *Desalin. Water Treat.* 29 (2011) 96–102.
- [32] J. Oakes, P. Gratton, Kinetic investigations of azo dye oxidation in aqueous media, *J. Chem. Soc. Perkin Trans. 2* (1998) 1857–1864.
- [33] C. Bauer, P. Jacques, A. Kalt, Photooxidation of an azo dye induced by visible light incident on the surface of TiO₂, *J. Photochem. Photobiol. A: Chem.* 140 (2001) 87–92.
- [34] M.Y.A. Mollah, J.A.G. Gomes, K.K. Das, D.L. Cocke, Electrochemical treatment of Orange II dye solution—use of aluminum sacrificial electrodes and floc characterization, *J. Hazard. Mater.* 174 (2010) 851–858.
- [35] S. Pirillo, V. Pedroni, E. Rueda, Elimination of dyes from aqueous solutions using iron oxides and chitosan as adsorbents: a comparative study, *Quim. Nova.* 32 (2009) 1239–1244.
- [36] A. Bedoui, M.F. Ahmadi, N. Bensalah, A. Gadri, Comparative study of Eriochrome black T treatment by BDD-anodic oxidation and Fenton process, *J. Chem. Eng.* 146 (2009) 98–104.
- [37] L.S. Clescerl, A.E. Greenberg, A.D. Eaton, *Standard Methods for the Examination of Water and Wastewater*, 20th ed., American Public Health Association, Washington, DC, 1999.
- [38] M. Panizza, P.A. Michaud, G. Cerisola, C. Comninellis, Anodic oxidation of 2-naphthol at boron-doped diamond electrodes, *J. Electroanal. Chem.* 507 (2001) 206–214.
- [39] S.S. Bhattacharya, V.K. Garlapati, R. Banerjee, Optimization of laccase production using response surface methodology coupled with differential evolution, *New Biotechnol.* 28 (2011) 31–39.
- [40] A.R. Khataee, M. Zarei, L. Moradkhannejhad, Application of response surface methodology for optimization of azo dye removal by oxalate catalyzed photoelectro-Fenton process using carbon nanotube-PTFE cathode, *Desalination* 258 (2010) 112–119.
- [41] T. Velegraki, G. Balayiannis, E. Diamadopoulou, A. Katsaounis, D. Mantzavinos, Electrochemical oxidation of benzoic acid in water over boron-doped diamond electrodes: Statistical analysis of key operating parameters, kinetic modeling, reaction by-products and ecotoxicity, *J. Chem. Eng.* 160 (2010) 538–548.
- [42] T. González, J.R. Domínguez, P. Palo, J. Sánchez-Martín, E.M. Cuerda-Correa, Development and optimization of the BDD-electrochemical oxidation of the antibiotic trimethoprim in aqueous solution, *Desalination* 280 (2011) 197–197.